9-1981

Acoustic Microscopy of Curved Surfaces

R. D. Weglein
Hughes Research Laboratories

Acoustic Microscopy of Curved Surfaces

Abstract
The Metrology and Imaging modes of the acoustic reflection microscope are applied to spherically shaped specimens. Metrology is usually practiced by translating the specimen along the acoustic beam axis. This operation yields a measurement of the local Rayleigh velocity at a single location in the specimen plane. Imaging is accomplished through raster-scanning in the plane transverse to the beam axis. The two modes are, in effect, simultaneously employed when a nonplanar surface of' known curvature is scanned. The resulting image reveals nearly concentric rings with radial, periodic brightness variation, if the surface is spherical in shape. Stainless steel bearing balls of the type used in gyros are used to demonstrate the technique. It is suggested that the obtained images represent a two-dimensional map of elastic properties applicable to convex (bearing ball) and concave (bearing raceway) surfaces.

Keywords
Nondestructive Evaluation

Disciplines
Materials Science and Engineering

ACOUSTIC MICROSCOPY OF CURVED SURFACES

R. D. Weglein
Hughes Aircraft Company
Canoga Park, CA 91304

ABSTRACT

The Metrology and Imaging modes of the acoustic reflection microscope are applied to spherically shaped specimens. Metrology is usually practiced by translating the specimen along the acoustic beam axis. This operation yields a measurement of the local Rayleigh velocity at a single location in the specimen plane. Imaging is accomplished through raster-scanning in the plane transverse to the beam axis.

The two modes are, in effect, simultaneously employed when a nonplanar surface of known curvature is scanned. The resulting image reveals nearly concentric rings with radial, periodic brightness variation, if the surface is spherical in shape. Stainless steel bearing balls of the type used in gyros are used to demonstrate the technique.

It is suggested that the obtained images represent a two-dimensional map of elastic properties applicable to convex (bearing ball) and concave (bearing raceway) surfaces.

THE ESSENTIAL ELEMENTS OF THE REFLECTION ACOUSTIC MICROSCOPE (Figure 1)

Images are obtained by raster scanning (in the X-Y plane) the highly converging sound beam across a planar object using a tiny drop of an "immersion" liquid, usually water. The object is usually situated in the acoustic focal plane and the reflected signals containing acoustic information are displayed on a synchronized cathode-ray tube monitor screen or storage oscilloscope. The focused acoustic beam is formed by a polished hemispherical depression in the sapphire rod shown in the figure. A piezoelectric transducer, consisting of a sputter-deposited layer of zinc oxide, converts the acoustic energy to and from the electrical signals that are imaged on the television screen. The reflection acoustic microscope may be likened to a pulsed radar imaging system in which the target "flies" at constant altitude and speed. In this manner, images of surface as well as subsurface detail are obtained depending on the altitude (at or below the surface) at which the focal plane intersects the object (target). Range-gating (not shown in the diagram) is used to select the desired image pulse from a host of spurious signals generated within the sapphire rod.

BEARING GEOMETRY (Figure 2)

A typical rolling element bearing consists of bearing balls, outer and inner raceways, as is shown in Figure 2. The surface of the bearing ball is convex and spherical. The raceways exhibit both convex and concave surfaces of nearly cylindrical curvatures. Portions of a gyro bearing ball were sectioned and examined in the acoustic microscope, that operates in the pulsed reflection mode in the frequency range near 400 MHz.

THE EXPERIMENT (Figure 3)

Bearing balls were sectioned to provide a comparison of AMS results on both planar and spherical surfaces with different surface finish. The 3/32 inch diameter balls were of 52100 stainless steel. The bearing ball sections were cemented to a fused quartz plate using a low temperature wax.

A scanning electron micrograph of the mounted sections is shown in Figure 3. The ball sections with their planar faces up expose a Hughes-polished 52100 stainless steel surface. The section denoted by the arrow is mounted with the spherical surface pointing up, and, therefore, presents a conventionally lapped bearing ball surface for diagnostic inspection. The arrow points to the apex of the sphere where the measurements were made.

EXPERIMENTAL RESULTS - I (Figure 4)

Acoustic material signatures (AMS) for these two cases are shown in Figure 4. The solid curve represents the measurement on the planar (Hughes-polished) surface, while the dashed curve is for the spherical bearing surface. The AMS curves are the video-detected transducer output power variation with object translation along the lens axis z. The AMS is the result of interference between two component waves that are reflected from the substrate (bearing) into the coupling liquid (deionized water, $v = 1.5$ mm/μs) and are vectorially summed in the piezoelectric transducer. As was shown previously, in the AMS mode Rayleigh waves are launched and detected coherently. From the physical model that was developed to explain the acoustic material signature[1, 2], the AMS period Δz_n is proportional to the square of the mean Rayleigh velocity in the plane of the substrate material. The measured period averaged over all periods in the figure yields the Rayleigh velocity v_R directly as given by Equation 1:

$$v_R = (v_\ell \cdot f \cdot \Delta z_N)^{1/2} = 23.56\,(\Delta z_N)^{1/2} \quad (1)$$

where the frequency of 370 MHz has been assumed, and v_ℓ is the velocity in water. Measured and derived results from Figure 4 are listed in the table. It can be seen that some difference exists between the two measurements on surfaces that differ both in shape as well as in their preparation.

DISCUSSION (Figure 4 and Table)

1) The local Rayleigh velocity was measured in a 150 μm diameter spot.

2) Amplitude reduction in spherical surface AMS is caused by acoustic beam divergence from curved surface.

3) Rayleigh velocity difference is <u>not</u> caused by curvature.

4) Surface condition is not known but different on bearing surface and planar section.

5) The measured Rayleigh velocity on the bearing surface is 5 percent lower than on planar section. This is consistent with a postulated "softer" bearing layer that results from observed decarburation of the martensitic matrix of 52100 stainless steel, commensurate with precipitation of the harder carbide grains, that occurs during lapping at high temperatures[3].

6) The AMS further yields an upper limit for acoustic absorption α_{max} for 52100 stainless steel on the planar section, α_{max} = 0.12 dB/Rayleigh wavelength at 0.375 GHz.

7) The "skin depth" for Rayleigh waves in this experiment ($\lambda_R/2\pi$) is approximately 1.15 μm.

EXPERIMENTAL RESULTS - II

An acoustic image of the spherical bearing surface, taken with the acoustic microscope, is shown in Figure 5a. This raster-scanned micrograph was taken with the apex of the spherical bearing surface at approximately 40 μm inside the acoustic focal plane (see Figure 5b) at a magnification of 100X. The nominal focal distance of this acoustic lens was previously determined to be 450 μm. The image covers an area approximately 600 μm in diameter, as Figure 5b indicates. The same approximate area, imaged in a scanning electron microscope, is seen in Figure 5c. A number of common surface features, such as surface indentations and debris, are apparent in both acoustic and SEM micrographs.

Superimposed on this surface detail is a series of bright and dark circular regions, visible only in the acoustic micrograph. These nearly concentric rings, denoted by (1), (2), and (3) in Figure 5b, correspond to the similarly numbered peaks of the spherical surface AMS shown previously in Figure 4. The outer ring represents the annular surface approximately in the focal plane, while the inner two bright fields, (2) and (3), represent elastic information at 23 and 40 μm, respectively, in front of the focal plane.

The particular number of rings shown here is quite arbitrary. The number may be increased to a maximum that corresponds to the number of periods shown in Figure 4, merely by further translation of the bearing surface toward the acoustic lens.

DISCUSSION (Figures 5 and 6)

The generation of the concentric set of bright and dark rings in Figure 5a may be related to the corresponding peaks and valleys of the acoustic material signature of Figure 4 with the aid of the construction shown in Figure 6. The spherical surface (Figure 6a) is used as a transfer curve to convert the one-dimensional AMS curve (Figure 6b) into the two-dimensional AMS regional map shown in Figure 6c. The latter is, of course, a qualitative image as approximately inferred from the peaks and valleys of the acoustic material signature. A set of numbers relate spatially the peaks and valleys on the AMS to the corresponding rings of varying degrees of brightness.

Figure 5a, therefore, constitutes a regional map of the acoustic material signature on the bearing ball. Just as the null spacing in the AMS of Figure 4 yields Rayleigh velocity information locally on the surface, so does the radial spacing of the dark rings in Figure 5 yield the Rayleigh velocity in the two-dimensional plane. For example, the radial separation of the dark rings along any radial direction, denoted by Δr in Figure 5, corresponds to the AMS spacing Δz_N and is therefore a measure of the Rayleigh velocity in that direction. Any variation in Δr would therefore reveal a local change in stiffness, density, or a combination of these. In fact, some variation in the width of the dark rings is quite evident in the left side of the imaged region. However, the assignment of a quantitative interpretation must await a full physical characterization (e.g., layer etch and SEM examination) of the surface.

CONCAVE-CYLINDRICAL SURFACES (Figure 7)

The generation of a set of concentric rings of periodically varying brightness was postulated using the convex-spherical surface as a transfer curve. In a similar manner, the raster-scanned acoustic image of a concave-cylindrical surface may be postulated. Such a surface is closely related to the bearing raceway that together with balls constitutes a complete bearing. Figure 7 illustrates the generation of an acoustic image representing the concave raceway surface. The raceway in cross section (Figure 7a) shows a cylindrical surface in the plane of the bearing axis with radius not much larger than that of the bearing ball. The bearing surface is nearly cylindrical since the bearing radius is many times larger than the raceway radius. The predicted qualitative acoustic material signature map is shown in Figure 7c, as a linear bar pattern of alternating brightness but with a variable period dictated by the slope of the circularly cylindrical surface.

SUMMARY AND CONCLUSIONS

- Acoustic microscope was applied to NDE of gyro bearing balls.
- Spherical and planar surface layers of 52100 stainless steel were inspected.
- AMS and imaging modes were used to measure elastic properties.

- Rayleigh velocity and acoustic attenuation values were determined.
- N. D. depth profiling and grain distribution sizing appears possible.
- Concave (race) as well as convex (ball) surfaces may be inspected.
- A. M. is potential low cost NDE technique for Q. C. of bearings.

ACKNOWLEDGEMENT

Supported by DARPA Order No. 3578 under Contract No. F33615-78-C-5196.

REFERENCES

1) Weglein. R. D., "A Model for Predicting Acoustic Material Signatures", Appl. Phys. Lett., Vol. 34, No. 3, pp 179-181, Feb. 1979.

2) Parmon, W. and Bertoni, H. L., "Ray Interpretation of the Material Signature in the Acoustic Microscope", Electronic Letters, Vol. 15, No. 21, pp 684-686, Oct. 1979.

3) Baginski. W. A., "Phase 1 - A New Approach to Advance the State-of-the-Art of Liquid Lubricated Instrument Ball Bearings", Customer Contract No. 04-493431-FS-5, Prime Contract No. F33615-78-C-4196, July 1979. Appendix A to: Gardos, N. M., "Solid Lubricated Rolling Element Bearings - Semiannual Report No. 2", DARPA Order No. 3576, AFML Contract No. F33615-78-C-5196, Hughes Aircraft Company Report No. FR-79-76-1041, 15 August 1979.

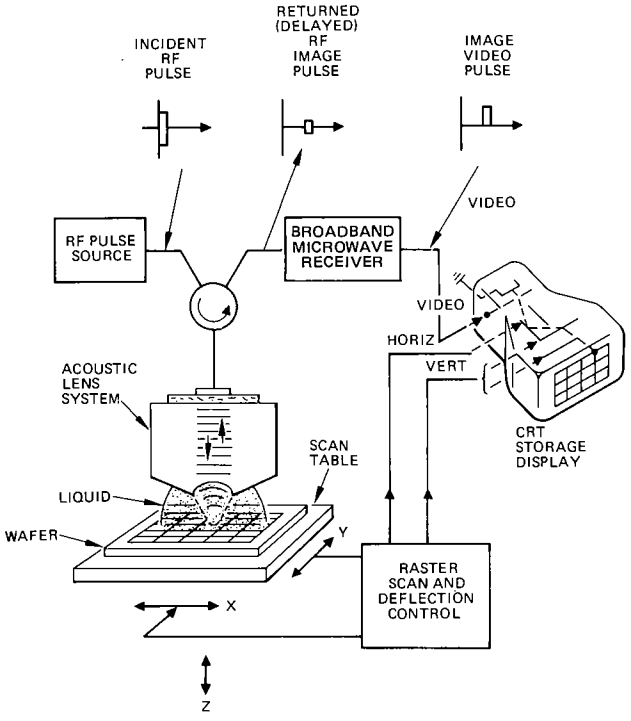

Figure 1. Schematic of Reflection Acoustic Microscope

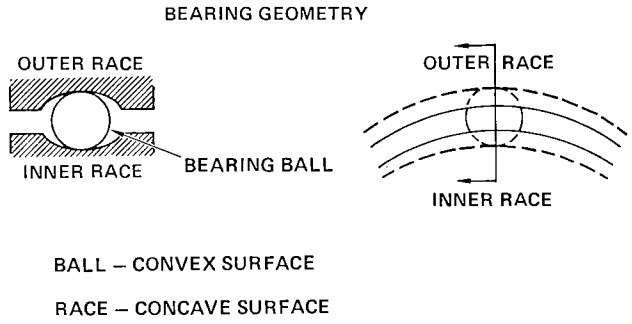

Figure 2. Bearing Geometry showing Convex (Ball) and Concave (Raceway) Surfaces

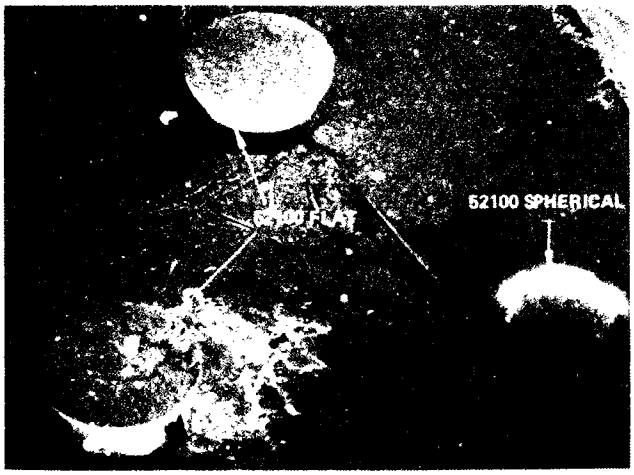

Figure 3. SEM Micrograph of Bearing Ball Sections Mounted for Diagnostic Inspection in Acoustic Microscope

TABLE. MEASURED RAYLEIGH VELOCITIES ON 52100 STAINLESS STEEL GYRO BEARING BALL

SURFACE	TYPE	Δz_N	v_R
		(μM)	MM/μSEC
PLANAR	GROUND AND POLISHED 52100 AT HUGHES	14.6	2.85
SPHERICAL	52100 CONVENTIONAL LAPPING BY BALL MANUF	13.2	2.71
PLANAR	NO. 347 STAINLESS STEEL		2.88*

*$v_R = \frac{0.87 + 1.12\sigma}{1 + \sigma} \cdot v_{sh}$; $\sigma_{347} = 0.30$; $v_{sh} = 3.10$ MM/μSEC

Δz_N = AMS PERIOD

v_R = MEAN RAYLEIGH VELOCITY

v_{sh} = SHEAR VELOCITY

σ = POISSON RATIO

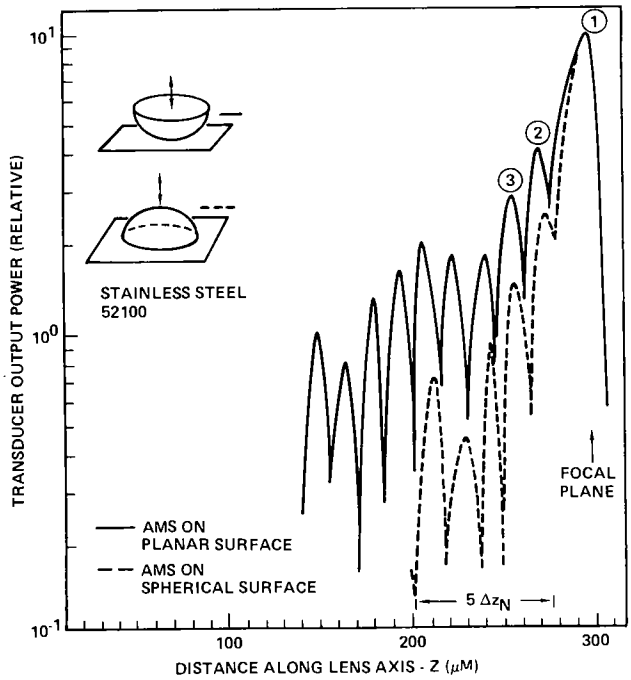

Figure 4. Acoustic Material Signatures on Planar and Spherical Surfaces

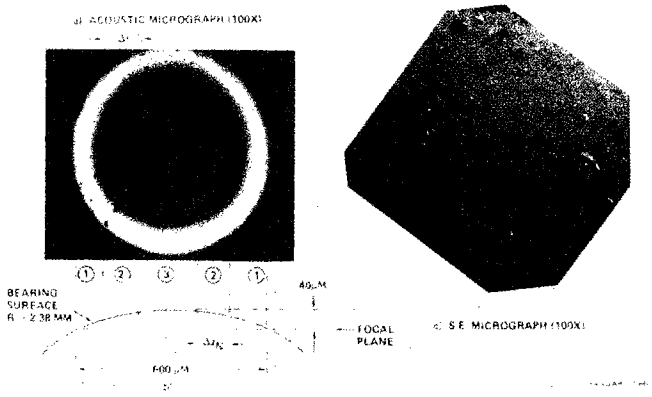

Figure 5. Acoustic and SEM Images of Gyro Bearing Ball Surface

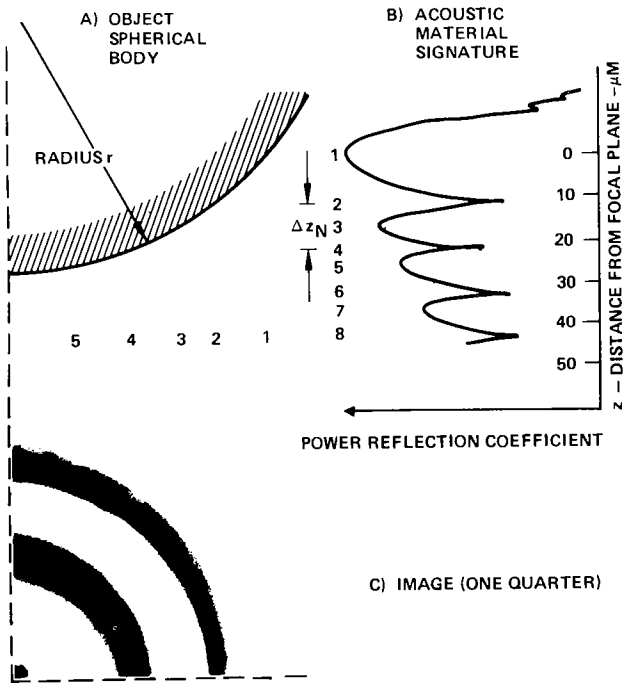

Figure 6. Acoustic Imaging of Convex Surface - Bearing Ball

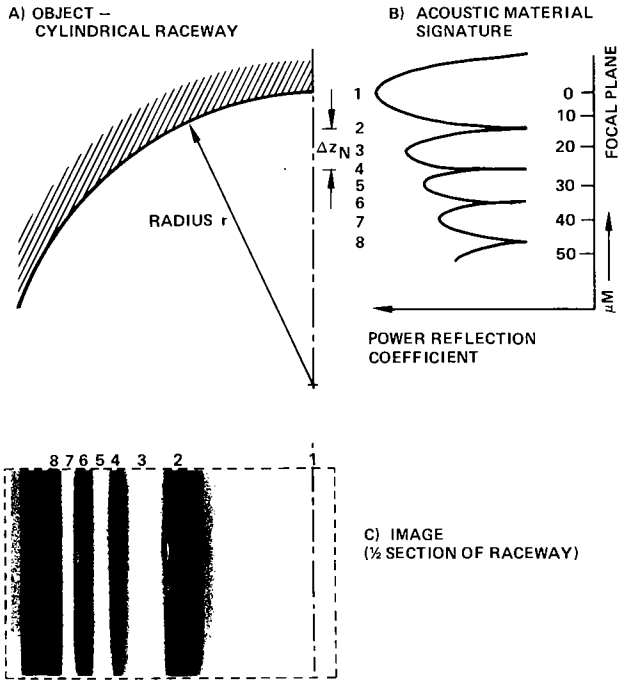

Figure 7. Acoustic Imaging of Concave Surface - Bearing Raceway